Quality Assessment of TanDEM-X Raw DEMs Oriented to a Fusion with CartoSAT-1 DEMs

Cristian Rossi, Michael Eineder, Thomas Fritz, Pablo D'Angelo and Peter Reinartz

German Aerospace Center (DLR), Remote Sensing Technology Institute (IMF), Oberpfaffenhofen, Germany; cristian.rossi@dlr.de

Abstract. This paper addresses a quality assessment of TanDEM-X standard raw DEMs, with a resolution of 12 meters, for two different terrain configurations: urban areas and moderate topography. The analysis is performed in the geospatial domain. Beside TanDEM-X, the same analysis is also carried out for CartoSAT-1 and LiDAR DEMs. The latter one is used as a reference. Nevertheless, the focus is centered on TanDEM-X, whose geometric limitations and their impacts on the DEM are analyzed here in detail. How the DEM appears in layover, shadow and phase unwrapping error areas is one of the objectives of the paper. The chosen test site is around Terrassa/Barcelona (Spain), offering all kinds of terrain variations. The final scope of the analysis is to learn about the potentials and the limitations of the two systems, radar (TanDEM-X) and optical (CartoSAT-1), in a way to optimally fuse them and to create an enhanced DEM. A simple fusion processing chain, based on a weighted average depending on the quality of the DEMs adapted to the local geometry, is tested. First results show that in urban areas the improvements are limited, mainly due to the previously analyzed geometrical issues, whereas in moderate terrain areas the enhancement is significant, with a drop in the RMSE of about 25% for TanDEM-X and 30% for CartoSAT-1.

Keywords. TanDEM-X, raw DEM, CartoSAT-1, DEM fusion.

1. Introduction

The TanDEM-X satellite has been launched in June 2010. Since that date, the mission has been scheduled to acquire data finalized to the generation of a global DEM following the HRTI-3 standards [1]. The TanDEM-X global DEM is generated by mosaicking and calibrating individual raw DEMs [2], having an average extension of 30 by 50 kilometers. At the Oberpfaffenhofen (Germany) processing facilities, the raw DEM production rate is particularly high (more than 500 raw DEMs per day). This large rate is made possible by using optimal algorithms in the raw DEM processing chain, embedded in a single processor named Integrated TanDEM-X Processor (ITP) [3].

The quality of the mosaicked DEM is continuously monitored [4]. In this paper, we investigate at the source of the errors looking at the quality of a standard raw DEM, having a resolution of about 12 meters. An assessment for a special case has been already performed in [5]. A height standard deviation of 6 meters has been reported for a high resolution urban DEM with 2.5 meters raster. In general, the quality of raw DEMs depends on many factors. First, the particular Synthetic Aperture Radar (SAR) geometry has a big impact in the DEM. Layover and shadow issues are intrinsic to the side-looking SAR geometry. The layover phenomenon occurs when the terrain slope exceeds the radar look angle causing a superposition, in a single resolution cell, of contributions coming from other areas. Shadow occurs when a region is not illuminated by the radar. The raw DEM profile for these areas is derived in [5]. Second, focusing and interferometric processing errors may manifest in the raw DEM in several forms. The interferometric coherence can be used for measuring these errors: it is simply the degree of correlation between the two images used for the raw DEM generation. Many inaccuracies can be included in this measure [1]. Nevertheless, it does not take into account errors manifesting after the interferogram generation in the processing chain.

Phase unwrapping inaccuracies are the biggest issues not considered in the coherence. They manifest in the raw DEM in height gradients proportional to the system height of ambiguity, an important parameter which triggers the performance. A way to detect these errors has been proposed in [6]. It makes use of the radargrammetric measurements employed in the coregistration processing stage as absolute reference.

The TanDEM-X mission is designed to mitigate raw DEM errors making use of a combination of several raw DEMs for the affected areas, in a dual-baseline approach [7]. In Sec. 2, we focus on the single-baseline raw DEM, investigating the discrepancies between TanDEM-X and a LiDAR reference in the geospatial domain. A CartoSAT-1 DEM processed at a 5 meters raster [8] is also analyzed. The chosen test site is around Terrassa/Barcelona (Spain), offering all kinds of terrain variations. Two DEM portions with different topography are studied. In Sec. 3, a simple DEM fusion based on the TanDEM-X and CartoSAT-1 geometrical proprieties is proposed and analyzed. The paper is concluded in Sec. 4 with a brief summary and an overview of future activities.

2. Quality assessment of TanDEM-X and CartoSAT-1 DEMs

The study is performed over the first two DEM patches used for the ISPRS benchmarking in [8]. The acquisition dates of the data used for the DEMs generation are November 2011 (TanDEM-X), February 2008 (CatoSAT-1) and November 2007 (LiDAR). The following assessment is based on the geometrical characteristics of the input DEMs, using approaches similar to the ones in [9]. For the analysis, the DEMs have been projected to the same grid (UTM, 10 meters raster). Nevertheless, it has to be noticed that the input resolution differs. TanDEM-X has the poorest resolution, of about 12 meters, whereas the CartoSAT-1 and the LiDAR resolutions are respectively 5 and 2 meters.

2.1. Terrassa, urban landscape

The first considered patch is over an urban area surrounded by smooth landscape. DEMs and relative geospatial maps are shown in Fig. 1. The first row contains the elevation models. The area, composed by a dense urban zone (northern part) and an industrial zone (center part), lies at the border of the TanDEM-X acquisition: the raw DEM does not fully cover the portion. A visual inspection of the DEMs and the geospatial maps shows how CartoSAT-1 has a better mapping of buildings compared to TanDEM-X, which results noisier. Moreover, buildings in TanDEM-X appear slightly shifted (wrongly geolocated), as visible from the error map in the fourth column. This is due to the layover mapping in the geocoding processing stage of TanDEM-X raw DEMs. In layover regions the raw DEM profile has been demonstrated to be a simple height ramp [5]. The buildings height and dimensions result generally underestimated and enlarged, respectively. Buildings lying in the vertical direction have a larger error [5]. The industrial area, composed by large structures, results better represented, with a comparable number of detected structures as in the reference.

Regarding CartoSAT-1, its urban mapping is over-performing the SAR sensor. Here, geometrical issues are less conspicuous. Occlusions may occur and small houses may be wrongly represented, but their effect in the DEM is less noticeable than the overall noise noticed for TanDEM-X.

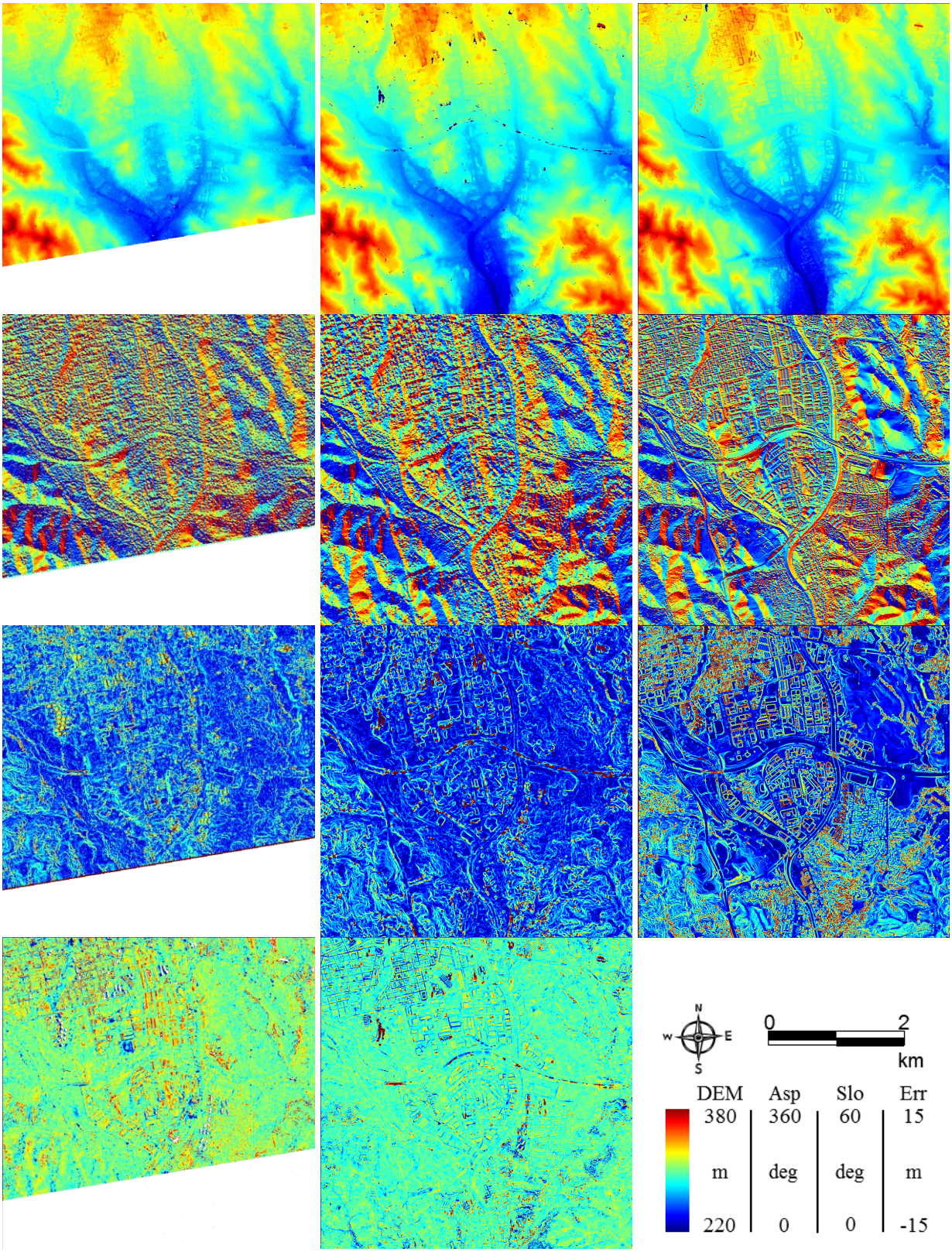

Figure 1. Terrassa geospatial maps for TanDEM-X (left column), CartSAT-1 (center column) and LiDAR (right column). The DEM portion, the aspect map, the slope map and the DEM difference with LiDAR are represented in the rows (first to fourth). The color scaling of the maps is at the bottom-right.

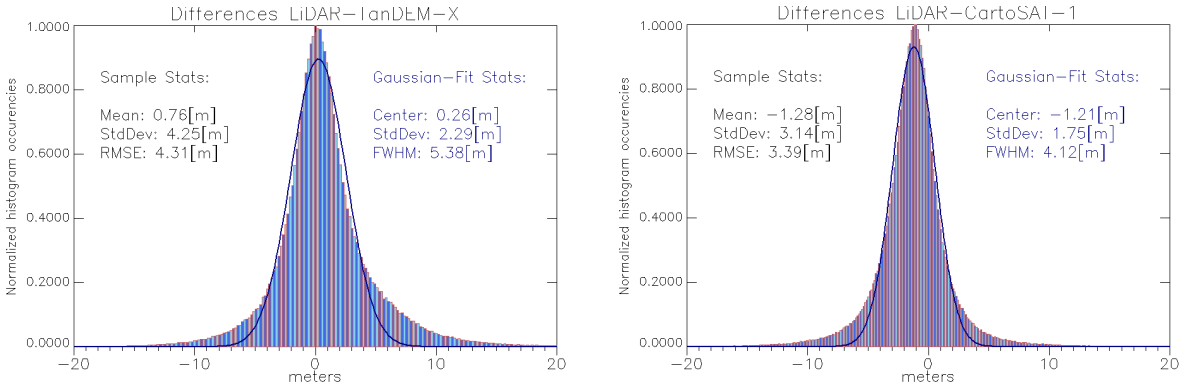

Figure 2. Terrassa test site: absolute differences between reference and TanDEM-X (left) and CartoSAT-1 (right) histograms.

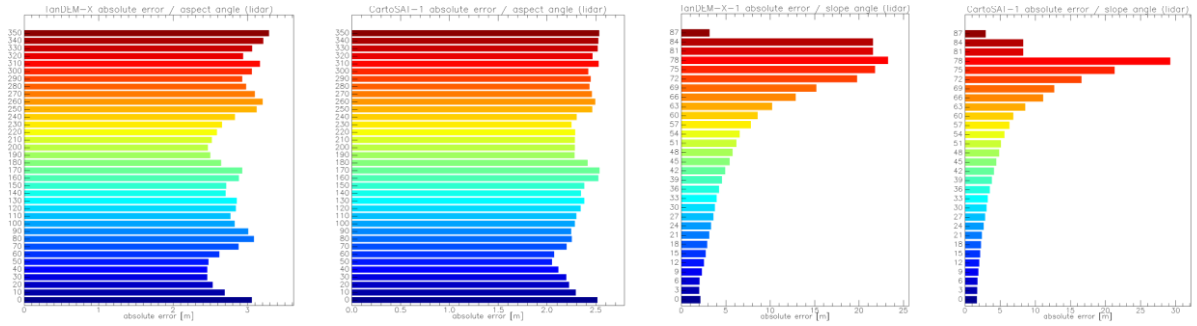

Figure 3. Terrassa test site: absolute error dependency for TanDEM-X aspect and slope (first and third) and CartoSAT-1 aspect and slope (second and fourth).

Only increasing the SAR resolution, i.e. adopting spotlight acquisitions, the results may be comparable. A contrast between the two DEMs is the presence of invalid pixels. In the CartoSAT-1 DEM, they are marked as dark blue points (Fig. 1, second column, first row). They are mainly located in the dense urban area, at the edge of some houses and on the main road. A skyscraper area at the north-west is fully invalidated. Contrariwise, a raw DEM value is always derived for TanDEM-X. This value may be inaccurate for low coherence areas: a map relating the standard height error to the measured coherence, called Height Error Map (HEM), is an ITP output [10]. Nevertheless, in case of urban areas, HEM is not fully matching the real standard error. This is due to layover zones, having high coherence when in both of the acquisitions the same layover component dominates – i.e. when the scattering of the wall fully dominates over the scattering of the roof or the ground, all contained in the same resolution cell.

In Fig. 2 the differences between the LiDAR reference and the DEMs under analysis are represented. Globally, CartoSAT-1 has better sample statistics, with a root mean square error drop of about 20% when compared to TanDEM-X. Regarding the absolute calibration, CartSAT-1 has more height overestimations whereas TanDEM-X has more underestimations, as previously explained (see also Fig. 1, fourth row). The calibration is a key issue for the interferometric reconstruction. In fact, a mis-calibration not only yields a global offset, but also geolocation errors [6]. This is not the case for optical matching algorithms.

In Fig. 3 the dependency of the errors with aspect and slope is represented. The slope dependency is similar for both of the cases, with higher errors for higher slopes. The aspect dependency slightly differs for north-east degrees, where TanDEM-X has higher errors due to shadowing.

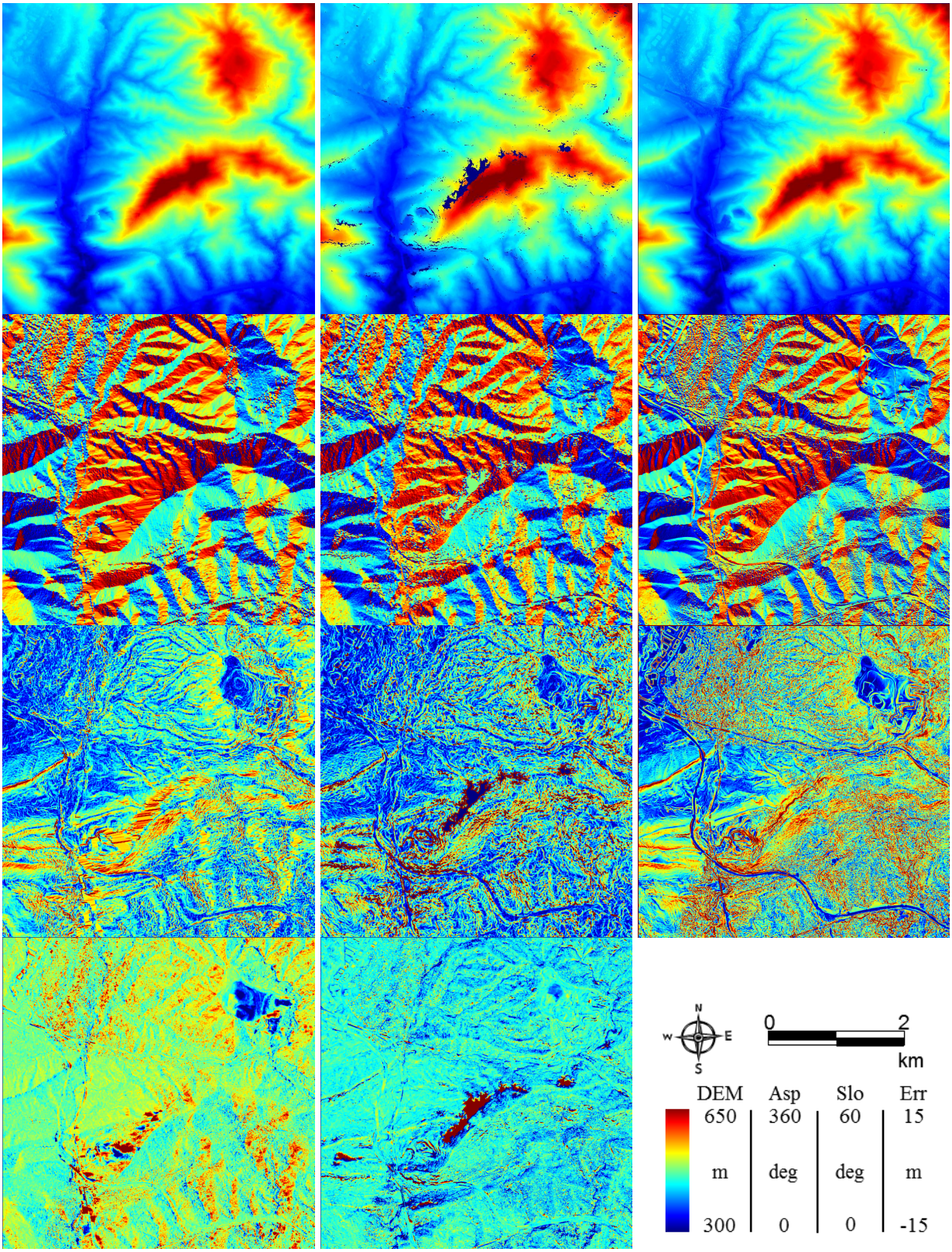

Figure 4. Vacarisses geospatial maps for TanDEM-X (left column), CartSAT-1 (center column) and LiDAR (right column). The DEM portion, the aspect map, the slope map and the DEM difference with LiDAR are represented in the rows (first to fourth). The color scaling of the maps is at the bottom-right.

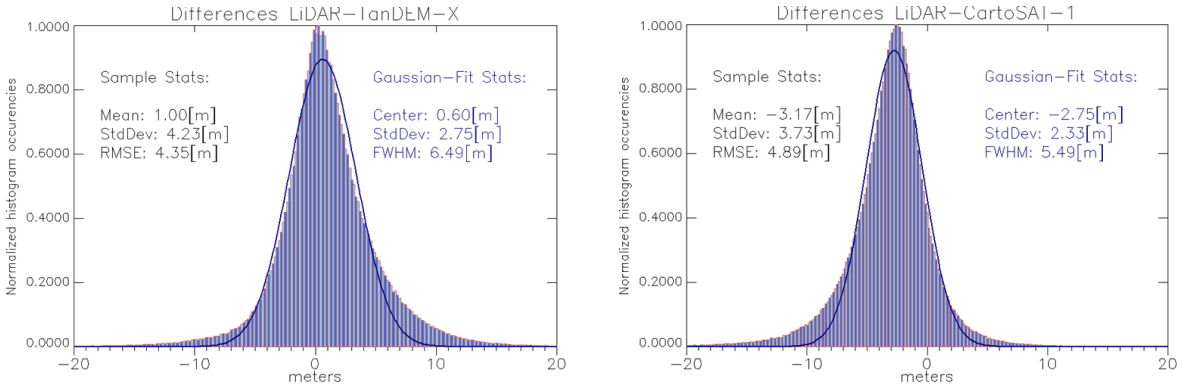

Figure 5. Valcarisses test site: absolute differences between reference and TanDEM-X (left) and CartoSAT-1 (right) histograms.

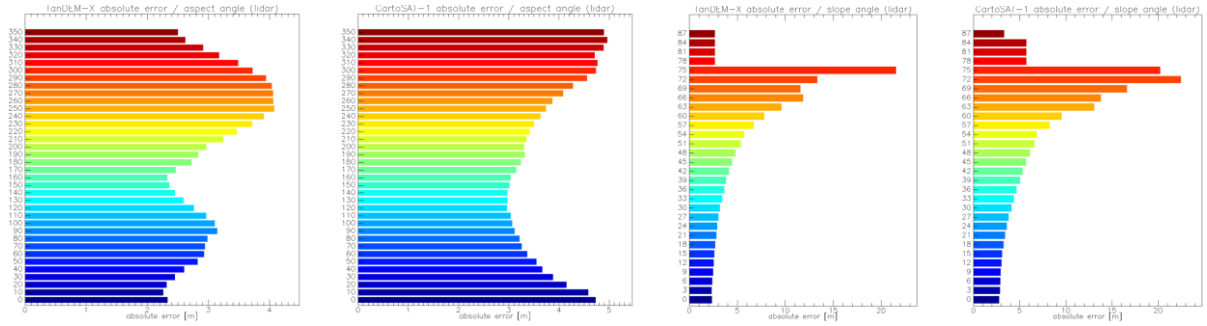

Figure 6. Valcarisses test site: absolute error dependency for TanDEM-X aspect and slope (first and third) and CartoSAT-1 aspect and slope (second and fourth).

2.2. Valcarisses, moderate terrain

The second test site for the benchmarking is composed by moderate terrain. The first row of Fig. 4 shows the DEMs. The patch is composed by a hill (center scene), an accumulation area (north-east), and an industrial area (north-west). The assessment follows the same strategy as in Sec. 2.1. A visual comparison of the elevation models does not reveal significant discrepancies as for the urban case. This is quantitatively demonstrated with the error histogram in Fig. 5. For this patch, TanDEM-X has a better RMSE, with a 10% drop compared to CartoSAT-1. As for the previous case, TanDEM-X underestimates the heights – due to layover areas – whereas CartoSAT-1 overestimates them, especially for high quotes. The absolute error is larger for CartoSAT-1. The accumulation area plays a role in the error particularly for TanDEM-X (Fig. 4, fourth row), having a 4 years temporal baseline with the reference, while CartoSAT-1 is much closer (4 months).

The western side of the hill is rather steep, with slopes larger than 60 degrees (Fig. 4, third column, third row). In this area there is the biggest concentration of CartoSAT-1 invalids. Since the western side is the one facing towards the SAR sensor, layover occurs for TanDEM-X. As for the previous patch, a height ramp is generated in layover zones (visible also in the aspect map of Fig. 4, first column, second row). In this case, the height error is proportional to topographic modulations around the height slope.

Interesting considerations can be made looking at Fig. 6. The error dependency with the slope is similar to the previous case – larger error for steeper terrain –. Instead, the dependency with the aspect shows a complementarity between TanDEM-X and CartoSAT-1. In particular, the TanDEM-X histogram results bimodal, with larger errors around two peaks, localized around the shadow aspect (first peak, easterly aspect) and the layover one (second and large peak, westerly aspect). Carto-

SAT-1 has instead larger errors for northerly aspect. Both of the sensors achieve the best performance for southerly aspect.

3. A quick DEM fusion approach

The two DEM sources can be combined in order to obtain an enhanced version of the elevation model. Several studies have been already performed (i.e. [12]). The DEM fusion basically relies on understanding the source of errors of the input map to fuse. As already pointed out, the TanDEM-X HEM is a powerful map to exploit. DEM samples with a large HEM should be discarded. They can be on water areas, shadow zones or dense forested areas where volume decorrelation occurs. Other samples to be discarded are the ones where phase unwrapping errors occur. They can be easily detected with a large threshold on the height difference between the two DEMs. The discrepancy is large as proportional to multiples of the height of ambiguity, having typical ranges of 40-50 meters for the mission. Invalid samples of the CartoSAT-1 DEM will be replaced by TanDEM-X, assuring that the replacement does not include phase unwrapping errors by checking the difference with a replacement by interpolation. Any other sample should be mixed following quality criteria. According to the considerations in Sec. 2, the complementarity of the sensors with respect to the aspect angle is an exploitable criterion. The dependency with the slope angle is less effective, since the sensors behave at the same manner. Nevertheless, training curves triggering the DEM sample weights are built. The first step is the absolute calibration of CartoSAT-1 to TanDEM-X, having a more accurate calibration. The complete algorithm is the following (CS stands for CartoSAT-1 DEM and TD for TanDEM-X raw DEM):

DEM fusion algorithm

1. Absolutely calibrate CS to the mean TD height
2. Replace CS invalid by linear interpolation
3. Check the difference between the filled invalid and TD. If (|difference| < HoA-***th1***), then use TD value
4. For every other sample, check the difference: d1 = |CS-TD|. If (d1> HoA-***th1***), then use CS sample and continue with the following sample from point 3, otherwise go to point 5.
5. Check the HEM value for the current sample. If larger than ***th2***, then use CS sample and continue with the following sample from point 3, otherwise go to point 6.
6. Perform a weighted average of the two DEM samples, depending on the current slope and aspect for both of the sensors and also on HEM for TD. In the average, CS and TD have a total weight depending on the scene to map. Moreover, the slope, aspect and HEM weights have also a different impact in the average. Continue with the following sample from point 3.

This simple algorithm is based on the use of thresholds and weights. The set of parameters employed for the Valcarisses benchmarking site is in Tab. 1. The aspect training curves are shown in Fig. 7. In Fig. 8 and Fig. 9 the results of the fusion are represented. The fused DEM results more accurate than the input DEMs (Fig. 5), with a better absolute calibration and a drop of the RMSE of about the 25% when compared to TanDEM-X and 30% when compared to CartoSAT-1. In contrast, the fusion result for the first benchmarking site, with the urban area of Terrassa, provides a smaller improvement, with a RMSE drop of 27% when compared to TanDEM-X and 7% for CartoSAT-1. The set of parameters for the first site are the same of the ones in Tab.1, except for the total weights, set to 75% for CartoSAT-1 and 25% for TanDEM-X due to the issues considered in Sec. 2.1. Nevertheless, large DEM problems as invalids or phase unwrapping errors are solved.

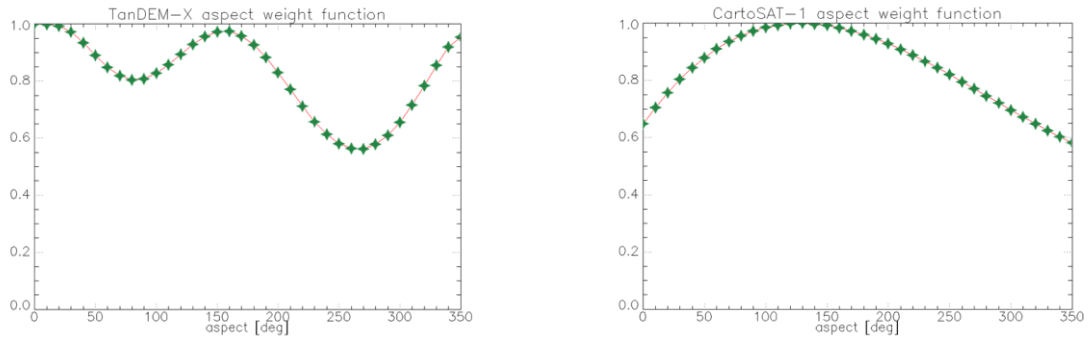

Figure 7. Aspect weight for TanDEM-X (left) and CartoSAT-1 (right)

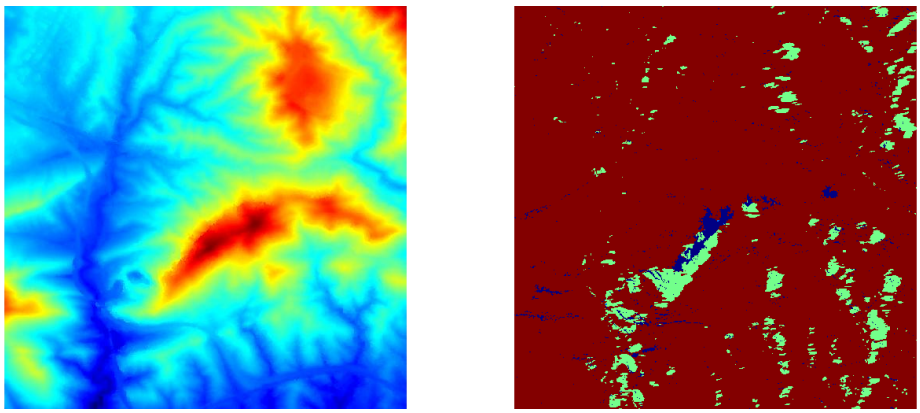

Figure 8. Valcarisses test site: fusion result (left) and fusion map (right). The colors in the map stand for weighted average (red), only CS/HEM threshold (green), only TD/CS invalid (dark blue), CS interpolation/CS invalid (light blue), only CS/TD phase unwrapping error (yellow).

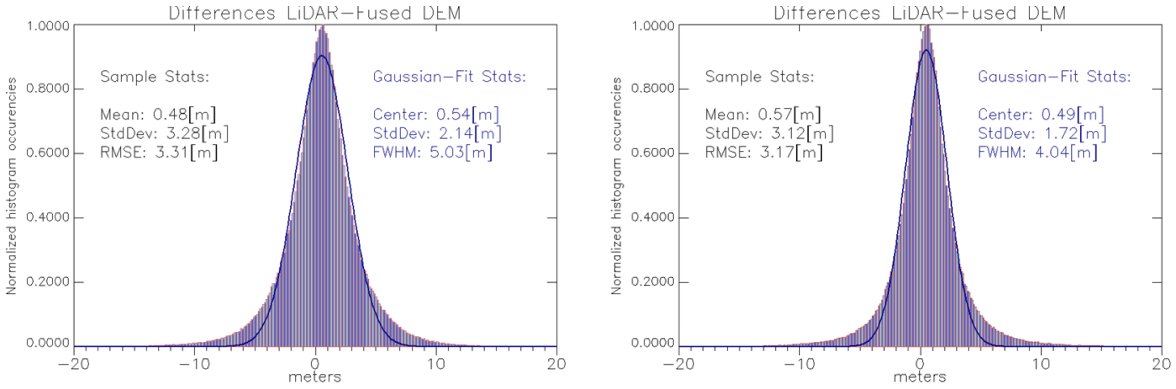

Figure 9. Histogram of the differences between reference and fused DEM for Valcarisses (left) and Terrassa (right).

Table 1. Parameters used for the DEM fusion (Valcarisses).

Parameter	**Value**	**Parameter**	**Value**
HoA	45m	CS aspect weight	60%
th1	10m	CS slope weight	40%
th2	2.5m	TD HEM weight	60%
total CS weight	50%	TD aspect weight	30%
total TD weight	50%	TD slope weight	10%

4. Conclusions

A first study on the quality of standard TanDEM-X raw DEMs and CartoSAT-1 DEMs oriented to their fusion has been proposed. The analysis has been carried out in the geospatial domain. For urban areas, the higher resolution of CartoSAT-1 and the lack of geometrical issues as layover let its globally better mapping when compared to TanDEM-X. Contrariwise, for moderate terrain the two sensors result comparable. TanDEM-X has a smaller RMSE in the considered test site. Accordingly, the fusion results significantly improve the sensors performance for non-urban areas, whereas for municipal zones the improvements are almost only for TanDEM-X. Future studies rely on more complex fusion algorithms and the exploitation of the spectral domain for the analysis.

References

[1] Krieger, G., Moreira, A., Fiedler, H., Hajnsek, I., Werner, M., Younis, M., Zink, M., 2007. TanDEM-X: A Satellite Formation for High-Resolution SAR Interferometry. IEEE Transactions on Geoscience and Remote Sensing 45 (11), 3317-3341.

[2] Gruber, A., Wessel, B., Huber,M., Roth, A., 2012. Operational TanDEM-X DEM Calibration and First Validation Results. ISPRS Journal of Photogrammetry and Remote Sensing 73, 39-49.

[3] Fritz, T., Rossi, C., Yague Martinez, N., Rodriguez Gonzalez F., Lachaise, M., Breit, H., 2011. Interferometric Processing of TanDEM-X Data. In: Proceedings of IEEE International Conference on Geoscience and Remote Sensing Symposium, IGARSS 2011, Vancouver, Canada, 24-29 July, pp. 2428-2431.

[4] Brautigam, B., Rizzoli, P., Martone, M., Bachmann, M., Kraus, T., Krieger, G., 2012. InSAR and DEM quality monitoring of TanDEM-X. In: Proceedings of IEEE International Conference on Geoscience and Remote Sensing Symposium, IGARSS 2012, Munich, Germany, 22-27 July, pp.5570-5573.

[5] Rossi, C., Gernhardt, S., Urban DEM generation, analysis and enhancements using TanDEM-X. ISPRS Journal of Photogrammetry and Remote Sensing (under review).

[6] Rossi, C., Rodriguez Gonzalez, F., Fritz, T., Yague Martinez, N., Eineder, M., 2012. TanDEM-X calibrated Raw DEM generation. ISPRS Journal of Photogrammetry and Remote Sensing 73, 12-20.

[7] Lachaise, M., Balss, U., Fritz, T., Breit, H., 2012. The Dual Baseline Interferometric Chain for the TanDEM-X Mission. In: Proceedings of IEEE International Conference on Geoscience and Remote Sensing Symposium, IGARSS 2012, Munich, Germany, 22-27 July, pp.5562-5565.

[8] d'Angelo, P., Reinartz, P., 2011. Semiglobal matching results on the ISPRS stereo matching benchmark. In: ISPRS Hannover Workshop 2011: High-Resolution Earth Imaging for Geospatial Information.

[9] Toutin, T., 2002. Impact of terrain slope and aspect on radargrammetric DEM accuracy, ISPRS Journal of Photogrammetry and Remote Sensing 57, 228-240.

[10] Rossi, C., Eineder, M., Fritz, T., Breit, H., 2010. TanDEM-X Mission: Raw DEM Generation. In: Proceedings of 8th European Conference on Synthetic Aperture Radar, EUSAR 2010, Aachen, Germany, 7-10 June, (on CD-ROM).

[11] Hoja, D., Reinartz, P., Schroeder, M., 2006. Comparison of DEM generation and combination methods using high resolution optical stereo imagery and interferometric SAR data. In: Proceedings of the ISPRS Commission I Symposium "From Sensors to Imagery", pp. 1682-1777.